Available online www.unicrossjournals.com
UNICROSS JOURNAL OF SCIENCE AND TECHNOLOGY, UJOST
RESEARCH ARTICLE VOL. 3(2) JUNE 30, 2024 ISSN:2814-2233
Date Approved June 30, 2024 Pages 54 - 64

VALIDATION OF CFD MODEL FOR TWO-PHASE GAS-LIQUID FLOW THROUGH A HORIZONTAL ANNULUS.

NYONG, O. E AND IGBONG, D.I.
Thermofluid, Combustion and Energy System Research Group, Department of Mechanical Engineering, University of Cross River State, Calabar, Nigeria.
Corresponding author: nyong.oku@unicross.edu.ng.

Abstract
The hydrodynamic behavior of different pipeline configurations such as vertical, horizontal, and inclined pipelines have been extensively studied. Flow patterns in concentric horizontal annuli, on the other hand, have gotten very little attention. The ability to precisely characterize multiphase flow patterns using computational techniques is crucial for the production, transportation facilities, and optimization of well designs. Using the capability of Ansys Fluent, the volume of fluid (VOF) multiphase model based on the Eulerian - Eulerian approach in conjunction with the turbulence models (Realizable k-ε) were used to model a two-phase flow regime such as dispersed bubble, elongated bubble, and wavy slug in a horizontal annulus. This work numerically predicts the flow regimes in a concentric horizontal annulus and then compared the simulated result with that of the visual observation obtained from the experimental high-speed camera. The simulations were performed on a test section of a 10.8 m length pipe with a hydraulic diameter of 0.0168 m using air and water as the working fluids. The visual observation from the experimental high-speed camera with the simulated flow pattern was seen to be in good agreement.

Keywords: elongated bubble flow, gas-liquid flow, liquid holdup, CFD modelling.

1.0 Introduction.

In oil and gas facilities, flow parameters like flow pattern, liquid holdup, and pressure drop are observed and must be precisely predicted when constructing production systems as well as maintaining and running downstream facilities in the horizontal annulus. These parameters enhance a reliable design for a multiphase flow pipeline and the engineer can develop the pipeline operations in the best possible way by having a thorough knowledge of the flow characteristic being demonstrated in a domain. This pattern of multiphase two-phase flow, like liquid-gas or liquid-liquid systems, which is more frequently found in facilities, enables discrete phases of flows to disperse into different regions within a conduit; this spatial dispersion is referred to as flow patterns or regimes.

These flow patterns are influenced by a number of factors, such as pipe geometry (Abdulkadir, 2011; Crawford et al., 2007) , fluid parameters (Sarica et al., 2013) and the conditions of flow, which were reported to influence the flow pattern or regime (Waelchli & von Rohr, 2006). The work of (Ekberg et al., 1999) revealed the impact of pipe geometry in a narrow horizontal annulus where the flow pattern was tested on two different annuli. The first pipe geometry of inner diameters (Di) and outer diameter (Do) of 0.0066 m and 0.00863m respectively. While the second pipe geometry of inner diameters (Di) and outer diameter (Do) of 0.03315 m and 0.0352 m respectively (Ekberg et al., 1999). Plug, slug, distributed bubble, churn, and other hybrid regimes were among the outcomes they got in their studies. Previous studies have shown that the center pipe's flow obstruction causes the flow structure in the annuli

configuration to differ from that of circular pipes (Eyo & Lao, 2019; Mahood et al., 2009). Additionally, compared to vertical flow, the gravity effect causes the annulus with horizontal geometry to exhibit more complex flow behavior (Barnea et al., 1983). Thus, the various flow regimes have distinct characteristics. However, flow characteristics in unrestricted channels have been extensively studied experimentally (Ismail et al., 2015; Mandhane et al., 1974) alongside vertical (Farman Ali & Yeung, 2015) and inclined pipelines (Barnea et al., 1980; Jagan & Satheesh, 2016; Rodriguez & Baldani, 2012). In horizontal annulus settings, the most common flow regimes captured by high-speed camera photography are dispersed bubble, elongated bubble, slug, wavy slug, churn, wavy annular, and annular (Eyo & Lao, 2019; Fakorede et al., 2021). Annulus eccentricity has shown to have tremendous effect on the shape and structure of the wavy annular, elongated bubble, and annular flow regimes (Eyo & Lao, 2019; Ibarra et al., 2019). The transition from an elongated bubble to a dispersed bubble may occur at high liquid superficial velocities (Eyo & Lao, 2019; Lage et al., 2000). In comparison, fully eccentric annulus, as opposed to concentric annulus, cause the transitions between various flow regimes to happen at higher liquid and lower gas superficial velocities (Eyo & Lao, 2019). Flows in totally eccentric annuli have a more well-defined structure than concentric annuli. However, the concentric annulus results in a greater pressure drop than the completely eccentric annulus (Ibarra et al., 2019). It is important to note that most research done prior to 2000 had limitations on data and application ranges (Lahiri & Ghanta, 2007). However, one of the most popular tools used for examining and characterizing flow regimes in complex geometries is CFD. The physics of the flow, the accessibility of computational resources, the level of accuracy required, and the time needed for the solution all have an impact on the fidelity of the results and the selection of turbulence model for a CFD problem. The usefulness of well-known Reynolds-averaged Navier-Stokes (RANS) turbulence models, that is, the k- ε model, k- ω model, and RSM in addition to large eddy simulation (LES) of steady fluid flow via pipelines has considerably been investigated in literature (Markatos, 1986; Sultan, 2018; Vijiapurapu & Cui, 2010). A numerical 3-dimensional (3D) study was investigated by (Gouidmi et al., 2019) on two-phase flow through in upward vertical concentric annular pipe. They implemented the VOF model, and k-ε model turbulence (Nyong et al., 2023). In their research, they observed global flux structures and transition regimes such as bubble size and shape, slug and their zigzag and coalescence phenomena (Nyong et al., 2023). Air velocity was seen to have significant impact on the flow regimes, and their findings validated the experimental data.
(Kiran et al., 2020) investigated two-phase flow in a vertical annulus using both experimental and modeling methods. Their model entails using two turbulence models (realizable k- ε and SST k-ω models) coupled with VOF multiphase model to simulate the pressure drop, void fraction, and flow regime. Their model's prediction and the experimental result agreed rather well, with a mean error of 20%. (Fakorede et al., 2021) numerically studied the CFD analysis of the liquid holdup and flow regime in annulus section. They implemented the VOF multiphase model couple with the turbulence models (Realizable k-ε) to predict liquid holdup and flow pattern. Within the studied condition U_{SG} = 0.18m/s and U_{SL} = 1.94m/s. At the top of the annulus cross-section, they noticed the dispersed bubble flow, which is composed of tiny gas bubbles dispersed throughout a continuous liquid phase. The model validation of horizontal annulus configurations and flow regime features has received relatively little research. The vast majority of descriptions of flow regimes universally relied on experimental evidence (Ekberg et al., 1999; Eyo & Lao, 2019; Sorgun et al., 2013), analytical models (Osgouei et al., 2010) and mechanistic models (Abbasi & Baniamerian, 2014; Barnea et al., 1980; Ozbayoglu & Omurlu, 2007) , where the flow channel's unusual shapes obstructed and deformed vision, making the experiment difficult. Model validation is critical in the construction of a piping system.
The purpose of this research is to carry out a CFD analysis of gas–liquid two phase annular flow to characterize the flow patterns in a horizontal annular pipe, that is., a configuration experimentally studied by (Eyo & Lao, 2019).

2.0 Geometrical Domain

The geometry for the model was prepared in ANSYS workbench. The model has two

sections. The first section is made of a stainless of length 2 m and the section proceeding the 2 m section is a transparent pipe with length of 10.8 m. The mixtures (gas and liquid) are injected separately into this pipe via the inclined pipe at 90^{O}. The pipe carrying gas inclined to the 2 m stainless steel pipe. The representation of the geometrical domain includes two sections for admitting gas and water into the test facility as described by (Eyo & Lao, 2019). When the gas and liquid enters into the pipe, both phases are premixed along the 2m length pipe before entering into the annulus section. This arrangement was accommodated to allow for a fully developed flow along the axial direction as detailed in the experimental setup and earlier suggested by previous research (Laufer, 1954). At the inlet of the annulus section is hydraulic diameter of 0.0168 m. Figure 1(a & b) shows the model used in the simulation in 3D. The pipe roughness height was considered to be 0.000015m for the wall, while the roughness constant was taken as 0.5. The gas-liquid phases were maintained at a room temperature of 273 K and atmospheric pressure of 1bar. The superficial gas-liquid velocities for the conditions studied ranges from 0.18 to 0.62 m/s and 0.28 to 1.94 m/s respectively. It is significant to know that the exact experimental features were replicated in the model found in the literature (Eyo & Lao, 2019).
Figure 1.0 depicts the geometry of the test section of the facility.

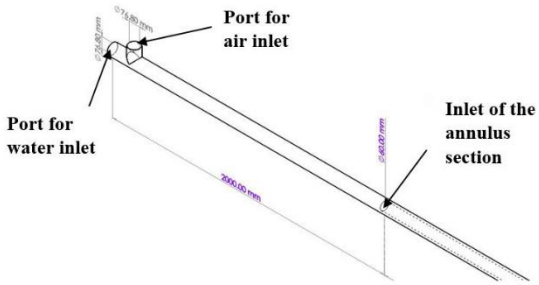

Figure 1. shows the 3 Dimensional (3D) isometric views of the test section of the facility

The parameters for the simulation were obtained from the previous work of (Eyo & Lao, 2019) which is displayed in Table 1.0.

Table 1: The parameters for the simulation [20].

S/N	Geometrical parameters	Values
1	diameter of the outer pipe section (m)	0.0768
2	diameter of the annulus section (m)	0.060
3	Hydraulic diameter	0.0168
4	Length of mixing section (m)	2
5	Length of annulus section (m)	10.8

At the entrance, velocities for gas-liquid phases were denoted to as superficial velocities for gas and superficial velocities for water respectively. While at the outlet is denoted by pressure outlet. The phases are defined with the primary phase as air and the secondary phase as water. At the entrance, both the density and the volume fraction of each phase were specified. The properties of gas and liquid are given in Table 2.

Table 2 shows superficial velocities and the properties of the fluid.

Cases	U_{SL} (m/s)	U_{SG} (m/s)	ρ_L (kg/ms)	ρ_G (kg/ms)
1	1.94	0.18	0.000894	0.00001821
2	0.27	0.21		
3	0.28	0.62		

2.1 Mesh study

The outcome of the simulation relies on the mesh characteristics. In the current study, the mesh sensitivity was carried out to ensure that the solution is independent of the mesh

resolution and also determine the minimum mesh density required to run the simulation to save computational time. Refined meshes was concentrated at the test section of the geometry which is the annulus section. Figure 2(a). shows the top and side view of the annulus section which has an inner and outer diameter of 0.06 m and 0.0768 m respectively. The top view of the annulus section shows how the inner and outer walls where structured mesh was adopted by retaining the finer mesh at the near wall region and reasonably coarser mesh at the central region of the annulus. Figure 2(b) also show the 3D symmetrical section where the mesh at the inlet section of the annulus and the symmetrical section are displayed structured mesh with refinement of mesh at the wall region. The mesh quality as indicated by the minimum orthogonal quality was about 0.998 which signifies a very good mesh.

The meshes were tested at a condition of superficial flow velocities of U_{SL} = 1.94 m/s and U_{SG} = 0.18 m/s respectively. Fluid density for liquid (ρ_L = 0.000894 kg/ms) and gas (ρ_G = 0.00001821 kg/ms). The properties of fluid and gas used in the simulation could be found in Table 2.

Figure 2. shows mesh at the cross section of the annulus pipe.

The mesh sensitivity study was carried out using the different mesh sizes that are depicted in Figure 3.

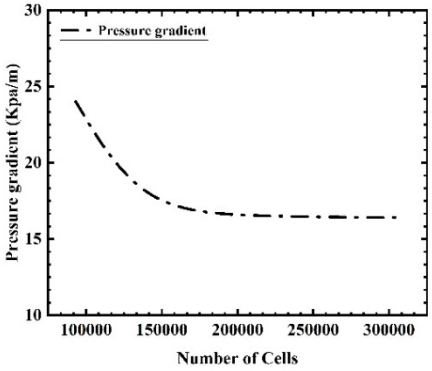

Figure 3 shows the mesh sensitivity analysis (Nyong et al., 2023).

The mesh sensitivity study was performed with mesh sizes up to 306000 cells as depicts in Figure 3. The figure showed a decline in the pressure as the mesh density is increased from 93,200 cells 205,000 cells whereas further increase in the volume of cells resulted to no significant change in the pressure gradient (Nyong et al., 2023). As a result, the flow solution and the integrated quantities will not be altered even if the number of mesh cells used to model the flow is increased beyond this volume of cells. Therefore, the mesh/cell sizes between 205,000 and 306,700 was found adequate to have no significant change in the pressure gradient as depicts in Figure 3.

2.2 Computational method

The conservation equations can be derived by averaging the local instantaneous balance for each phase (Anderson & Jackson, 1967), or the mixture theory method could be applied (Atkin & Craine, 1976; Bowen, 1976). If the phase is q then

The phase volume V_q is given as

$$V_q = \int X_q dV \tag{1}$$

$$\sum_{q=1}^{n} X_q = 1 \tag{2}$$

Where X_q is the volume fraction phase. For continuity equation of the phase q is represented as:

$$\frac{\partial}{\partial t}\left(\rho_q X_q\right)+\nabla.\left(\rho_q X_q \vec{u}_q\right)=0 \tag{3}$$

Where ρ_q, the volume is average density of the q^{th} phase in the solution domain and $\vec{u}_q$ is the velocity phase of q^{th}. The momentum equation for a fluid phase q is given as :

$$\frac{\partial}{\partial t}\left(\rho_q X_q \vec{u}_q\right)+\nabla.\left(\rho_q X_q \vec{u}_q \vec{u}_q\right)=-X_q \nabla P+\nabla.\bar{\bar{\tau}}_q+\rho_q X_q \vec{g}$$
$$+\sum_{p=1}^{n}\left(\vec{R}_{pq}+\dot{m}_{pq}\vec{u}_{pq}-\dot{m}_{qp}\vec{u}_{qp}\right)$$
$$+\left(\vec{F}_q+\vec{F}_{lift,q}+\vec{F}_{td,q}+\vec{F}_{wl,q}+\vec{F}_{vm,q}\right) \tag{4}$$

Where P is the pressure shared by the entire phase, $\bar{\bar{\tau}}_q$ is the q^{th} phase stress-strain tensor, $\vec{g}$ is the acceleration due to gravity, $\dot{m}_{pq}$ is the mass flow from (q to p) phase, $\vec{F}_q$ is the external body force, $\vec{F}_{lift,q}$ is the lift force, $\vec{F}_{td,q}$ is the turbulence dispersion force, $\vec{F}_{wl,q}$ is the wall lubrication force and $\vec{F}_{vm,q}$ is the virtual mass force.

The drag term, which dominates all other interfacial terms, is defined in equation 5 as:

$$\sum_{p=1}^{n}\vec{R}_{pq}=\sum_{p=1}^{n}K_{pq}\left(\vec{u}_p-\vec{u}_q\right) \tag{5}$$

Where $K_{pq}=K_{qp}$ is the interface exchange coefficient given as

$$K_{qp}=\frac{X_q X_p \rho_q f}{\tau_q} \tag{6}$$

Here f is the drag function which has the drag coefficient and it's dependent on the Reynolds number. Assuming no mass transfer occurs, the gaseous phase is referred to as the dispersed phase, while the liquid phase is represented as the continuum and the governing equations (continuity and momentum) for the gas phase is given in equation (7) (Launder & Spalding, 1983).

$$\frac{\partial}{\partial t}\left(\rho_g X_g \vec{u}_g\right)+\nabla.\left(\rho_g X_g \vec{u}_g \vec{u}_g\right)=-X_g \nabla P+\nabla.\bar{\bar{\tau}}_g+\rho_g X_g \vec{g}$$
$$+\sum_{p=1}^{n}\left(\vec{R}_{lg}+\dot{m}_{lg}\vec{u}_{lg}-\dot{m}_{gl}\vec{u}_{gl}\right)$$
$$+\left(\vec{F}_g+\vec{F}_{lift,g}+\vec{F}_{td,g}+\vec{F}_{wl,g}+\vec{F}_{vm,g}\right) \tag{7}$$

Where X_g and X_l are the volume fractions for gas and liquid respectively.

Equation (8) gives the lift force in terms of the slip velocity and the curl of the liquid phase velocity.

$$\vec{F}_{lift,g}=-C_l \rho_g X_g\left(\vec{u}_l+\vec{u}_g\right)\times\left(\nabla\times\vec{u}_l\right) \tag{8}$$

The wall lubrication force equation is written as:

$$\vec{F}_{wl,g}=C_{wl}\rho_l X_l\left(\vec{u}_l+\vec{u}_g\right)_{\|}\,|\,\vec{n}_w \tag{9}$$

The Realizable k-epsilon (k-ε) turbulence model developed by Launder and Spalding [45] with standard wall functions was implemented in the ANSYS code to solve the flow problem. The kinetic energy of turbulence is calculated using these transport equations k, and its rate of dissipation, ε, respectively and are given in following equation (10) and (11) (Manual, 2009):

$$\frac{\partial}{\partial t}(\rho k)+\frac{\partial}{\partial xi}(\rho k u_i)=\frac{\partial}{\partial xj}\left[\left(\mu+\frac{\mu_t}{\sigma_k}\right)\frac{\partial k}{\partial x_j}\right]$$
$$+G_k+G_b-\rho\varepsilon-Y_M+S_k \tag{10}$$

and

$$\frac{\partial}{\partial_t}(\rho\varepsilon)+\frac{\partial}{\partial x_i}(\rho\varepsilon u_i)=\frac{\partial}{\partial x_j}\left[\left(\mu+\frac{\mu_t}{\sigma_\varepsilon}\right)\frac{\partial\varepsilon}{\partial x_j}\right]$$
$$+C_{1\varepsilon}\frac{\varepsilon}{k}\left(G_k+C_{3\varepsilon}G_b\right)-C_{2\varepsilon\rho}\frac{\varepsilon^2}{k}+S_\varepsilon \tag{11}$$

Where G_k, G_b, Y_M are generation of turbulence kinetic energy as a result of the mean velocity gradients, turbulence kinetic energy due to buoyancy, and the contribution of the fluctuating dilatation in compressible turbulence to the overall dissipation rate

respectively. $C_{1\varepsilon}$, $C_{2\varepsilon}$, and $C_{3\varepsilon}$ are the constants, σ_k, and σ_ε are turbulent Prandtl numbers for k and ε respectively while the source terms are represented as S_k and S_ε.

In the current simulation, at the walls, the conditions were assumed to be non-slip at V = 0, and the approach of the wall function was used. A pressure-based solver was in use where the governing equations were discretized adopting the finite volume method. Semi-Implicit Method for Pressure-Linked Equations (SIMPLE) scheme was utilized for pressure-velocity coupling calculations . The First Order implicit scheme was adopted for the transient formulation. The inlet flow conditions were initialized using the usual initialization procedure. The liquid phase was patched throughout the entire flow domain after initiation. 100 iterations were permitted for each step, with a time step of 0.001s, which satisfy the convergence criteria. The standard convergence criterion of 0.001 was selected for residuals of continuity, velocity (u, v, w), kinetic energy (k) and dissipation rate (ε). Flow time was used to track parameters such as volumetric average liquid holdup and pressure gradient. The area weighted average of the liquid holdup fraction distribution was captured in order to further characterize the flow pattern that was observed in the modelling.

3.0 Results and Discussions

3.1 Dispersed bubble flow

Figure 4 (a) depicts the calculated contour volume of liquid holdup at the condition studied at U_{SG} = 0.18 m/s and U_{SL} = 1.94 m/s. The CFD results in Figure 4 (a) depicts that the dispersed bubble flow regime is detected, as shown in the contour of volume fraction of water. A large number of dispersed bubbles can be seen near the top of the annulus area. These bubbles are created by the breaking of the slug and the movement of elongated bubbles along the annulus section. This effect results in significant liquid holdup values along the annulus region.

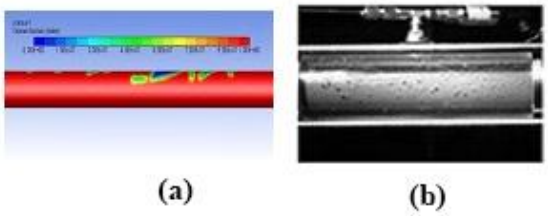

Figure 4 display comparison of simulated variation liquid holdup with the experimental observed image from high-speed camera for dispersed bubbles flow at U_{SG} = 0.18 m/s and U_{SL} = 1.94 m/s. (a) simulated variation liquid holdup (b) experimental observed image from high-speed camera (Manual, 2009).

3.2 Elongated bubble flow

Figure 5 (a) depicts the calculated contour volume of liquid holdup for the elongated bubble at U_{SG} = 0.27 m/s and U_{SL} = 0.21 m/s. According to the findings in Figure 5(a), within the region, the bubble flow is characterized by a discontinuous liquid body that fills the annulus zone and is limited at its top by gas plugs. As previously reported in literature (Andrianto et al., 2016; Caetano et al., 1992) at a lower gas and liquid superficial velocities, this particular flow pattern is significant and is characterized by an alternating liquid body that fills the entire cross section of the annulus and gas plugs confined at the annulus's top. The profile of the formed gas plug is rightly conditioned by the annulus configuration. When the result is compared with the image captured from the high speed camera in Figure 5(b). It is evident that the simulated contour volume of liquid holdup for the elongated bubble replicates the image captured by the experimental visualization.

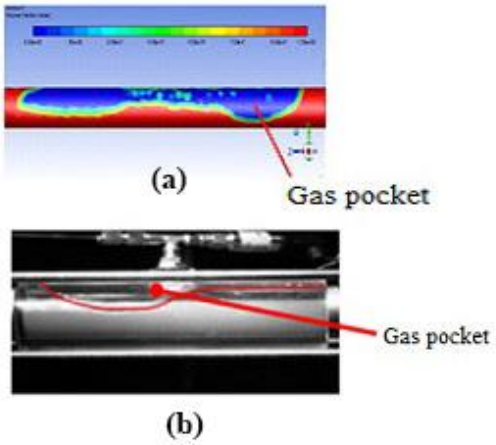

Figure 5 shows the comparison of model with experiment for elongated bubbles flow at U_{SG} = 0.27 m/s and U_{SL} = 0.21 m/s. (a) contour of volume fraction of water in the annulus section for an Elongated bubble flow (b) visual image from high speed camera (experimental) (Eyo & Lao, 2019; Nyong et al., 2023).

3.3 Slug flow

The CFD simulation is run for 15s, and liquid holdup data is recorded throughout the flow time. The slug flow pattern is captured after a fully developed flow was met, and an initial data of 3.5s was ignored before the liquid holdup data was recorded for the simulation. The condition for the superficial velocities of air and water are U_{SG} = 0.62 m/s and U_{SL} = 0.28 m/s respectively. At higher gas superficial velocities, the slug flow pattern is observed. Figure 7(a) depicts the simulated contour of volume fraction of water. It is clear that the air phase appears in two different forms: large and small spherical bubbles dispersed in the water phase. Large bubbles occupy almost the entire cross section of the annular surface and move uniformly upwards. The liquid (water) phase appears as liquid plugs that span the cross section of the annulus pipe. And as falling liquid films that flow downwards between the large bubbles (slugs air) and the tube walls. The slugs (water) which separate the main successive bubbles contain small dispersed spherical gas bubbles. As a result of a decrease in flow holdup and increased turbulence, the liquid phase wraps itself around the inner pipe of the annulus and contains some entrained air bubbles flowing close to the top of the annulus (Eyo & Lao, 2019). As a result of the high gas superficial velocity, presence of wavy interface and stratified smooth flow is preceded along the annulus section during the flow simulation. The contour phase distribution for the case in Figure 7(a) has shown a clear a chaotic, unstable and wavy spike image which behavior was equally reported by (Ibarra et al., 2019) . Similar trend was captured from the visual (experiment) image displaced in Figure 7(b).

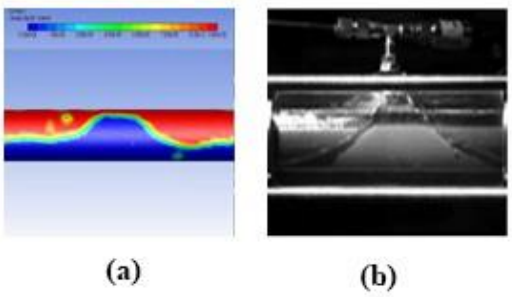

Figure 7 shows comparison of CFD model with the visualized (experimental) image of wavy flow at U_{SG} = 0.62 m/s and U_{SL} = 0.28 m/s. (a) Simulated contour of volume fraction of water within the annulus region for slug flow (b) visual (experiment) image observations from high-speed imaging (Eyo & Lao, 2019; Nyong et al., 2023).

4.0 Conclusion

The current work simulated the two-phase flow pattern utilizing the VOF multiphase model based on the Eulerian-Eulerian approach in conjunction with the turbulence models (Realizable k-ε) in Ansys Fluent. The simulations were done on a 10.8 m long pipe with a hydraulic diameter of 0.0168 m using air and water as the working fluids. For the condition of superficial velocity study, three basic two-phase flow regimes were observed. These flow patterns were obtained depending on the variation in air and water superficial velocities such as, the elongated bubble, dispersed bubble, and the wavy slug regimes.
When compared, the CFD models of contour volume of liquid with the obtained experimental image from the high speed camera, the model was seen to mimic the experimental flow pattern.

ACKNOWLEDGEMENT
Thanks to the Federal Government of Nigeria through the office of the Tertiary Educational Trust Fund (TETFUND) for sponsoring this research work through the Institutional Based

Research (IBR) grant. A final thank you to the Department of Mechanical Engineering, University of Cross River State where this research was carried out.

Reference

Abbasi, M., & Baniamerian, Z. (2014). Analytical simulation of flow and heat transfer of two-phase nanofluid (stratified flow regime). *International Journal of Chemical Engineering*, *2014*(1), 474865.

Abdulkadir, M. (2011). *Experimental and computational fluid dynamics (CFD) studies of gas-liquid flow in bends* University of Nottingham].

Anderson, T. B., & Jackson, R. (1967). Fluid mechanical description of fluidized beds. Equations of motion. *Industrial & Engineering Chemistry Fundamentals*, *6*(4), 527-539.

Andrianto, M., Widyaparaga, A., & Dinaryanto, O. (2016). CFD Studies on the gas-liquid plug two-phase flow in a horizontal pipe. *Journal of Petroleum Science and Engineering*, *147*, 779-787.

Atkin, R., & Craine, R. (1976). Continuum theories of mixtures: applications. *IMA Journal of Applied Mathematics*, *17*(2), 153-207.

Barnea, D., Luninski, Y., & Taitel, Y. (1983). Flow pattern in horizontal and vertical two phase flow in small diameter pipes. *The Canadian Journal of Chemical Engineering*, *61*(5), 617-620.

Barnea, D., Shoham, O., Taitel, Y., & Dukler, A. (1980). Flow pattern transition for gas-liquid flow in horizontal and inclined pipes. Comparison of experimental data with theory. *International Journal of Multiphase Flow*, *6*(3), 217-225.

Bowen, R. M. (1976). Continuum physics. *Theory of mixtrures*, 4.

Caetano, E., Shoham, O., & Brill, J. (1992). Upward vertical two-phase flow through an annulus—Part II: Modeling bubble, slug, and annular flow.

Crawford, N., Cunningham, G., & Spence, S. (2007). An experimental investigation into the pressure drop for turbulent flow in 90 elbow bends. *Proceedings of the Institution of Mechanical Engineers, Part E: Journal of Process Mechanical Engineering*, *221*(2), 77-88.

Ekberg, N., Ghiaasiaan, S., Abdel-Khalik, S., Yoda, M., & Jeter, S. (1999). Gas–liquid two-phase flow in narrow horizontal annuli. *Nuclear engineering and design*, *192*(1), 59-80.

Eyo, E. N., & Lao, L. (2019). Gas-liquid flow regimes in horizontal annulus. *Journal of Petroleum Science and Engineering*, *175*, 573-586.

Fakorede, D., Nyong, O., Ifere, M., Bepaye, A., Igbong, D., & Ebieto, C. (2021). CFD modelling of dispersed bubble two-phase flow in a concentric annulus pipe. *International Research Journal of Innovations in Engineering and Technology*, *5*(9), 82.

Farman Ali, S., & Yeung, H. (2015). Experimental study of two-phase air–water flow in large-diameter vertical pipes. *Chemical Engineering Communications*, *202*(6), 823-842.

Gouidmi, H., Benderradji, R., Beghidja, A., & Tayebi, T. (2019). Numerical study of upward vertical two-phase flow through an annulus concentric pipe. *Journal of Advanced Research in Fluid Mechanics and Thermal Sciences*, *58*(2), 187-206.

Ibarra, R., Nossen, J., & Tutkun, M. (2019). Two-phase gas-liquid flow in concentric and fully eccentric annuli. Part I: Flow patterns, holdup, slip ratio and pressure gradient. *Chemical Engineering Science*, *203*, 489-500.

Ismail, A. S. I., Ismail, I., Zoveidavianpoor, M., Mohsin, R., Piroozian, A., Misnan, M. S., & Sariman, M. Z. (2015). Experimental investigation of oil–water two-phase flow in horizontal pipes: Pressure losses, liquid holdup and flow patterns. *Journal of Petroleum Science and Engineering*, *127*, 409-420.

Jagan, V., & Satheesh, A. (2016). Experimental studies on two phase flow patterns of air–water mixture in a pipe with different orientations. *Flow Measurement and Instrumentation*, *52*, 170-179.

Kiran, R., Ahmed, R., & Salehi, S. (2020). Experiments and CFD modelling for

two phase flow in a vertical annulus. *Chemical Engineering Research and Design*, *153*, 201-211.

Lage, A. C., Rommetveit, R., & Time, R. W. (2000). An experimental and theoretical study of two-phase flow in horizontal or slightly deviated fully eccentric annuli. IADC/SPE Asia Pacific Drilling Technology Conference and Exhibition?,

Lahiri, S., & Ghanta, K. (2007). Computational technique to predict the velocity and concentration profile for solid-liquid slurry flow in pipelines. 17th International conference on hydrotransport, Capetown, South Africa,

Laufer, J. (1954). *The structure of turbulence in fully developed pipe flow*.

Launder, B. E., & Spalding, D. B. (1983). The numerical computation of turbulent flows. In *Numerical prediction of flow, heat transfer, turbulence and combustion* (pp. 96-116). Elsevier.

Mahood, H. B., Kadim, H. A., & Salim, A. N. (2009). Effect of Flow-Obstruction Geometry on Pressure Drops in Horizontal Air-Water Two-Phase Flow. *Al-Qadisiya Journal For Engineering Sciences*, *2*(3), 641-653.

Mandhane, J., Gregory, G., & Aziz, K. (1974). A flow pattern map for gas—liquid flow in horizontal pipes. *International Journal of Multiphase Flow*, *1*(4), 537-553.

Manual, U. (2009). ANSYS FLUENT 12.0. *Theory Guide*, *67*.

Markatos, N. (1986). The mathematical modelling of turbulent flows. *Applied Mathematical Modelling*, *10*(3), 190-220.

Nyong, O. E., Igbong, D. I., Ebieto, C. E., Ekpo Ene, B., Oluwadare, B., & Archibong Eso, A. (2023). Numerical simulation of two-phase gas-liquid flowthrough horizontal annulus pipe. *Archives of Thermodynamics*, *vol. 44*(No 4), 705-731. http://journals.pan.pl/Content/131168 http://journals.pan.pl/dlibra/publication/edition/131168 http://journals.pan.pl/Content/131168/PDF/art31.pdf

Osgouei, R. E., Ozbayoglu, E. M., Ozbayoglu, M. A., & Yuksel, E. (2010). Flow pattern identification of gas-liquid flow through horizontal annular geometries. SPE Oil and Gas India Conference and Exhibition?,

Ozbayoglu, M., & Omurlu, C. (2007). Modelling of two-phase flow through concentric annuli. *Petroleum science and technology*, *25*(8), 1027-1040.

Rodriguez, O., & Baldani, L. (2012). Prediction of pressure gradient and holdup in wavy stratified liquid–liquid inclined pipe flow. *Journal of Petroleum Science and Engineering*, *96*, 140-151.

Sarica, C., Pereyra, E. J., & Brito, R. (2013). Effect of medium oil viscosity on two phase oil gas flow behavior in horizontal pipes. Offshore Technology Conference,

Sorgun, M., Osgouei, R., Ozbayoglu, M., & Ozbayoglu, A. (2013). An experimental and numerical study of two-phase flow in horizontal eccentric annuli. *Energy Sources, Part A: Recovery, Utilization, and Environmental Effects*, *35*(10), 891-899.

Sultan, R. A. (2018). *A comprehensive study on multiphase flow through pipeline and annuli using CFD approach* Memorial University of Newfoundland].

Vijiapurapu, S., & Cui, J. (2010). Performance of turbulence models for flows through rough pipes. *Applied Mathematical Modelling*, *34*(6), 1458-1466.

Waelchli, S., & von Rohr, P. R. (2006). Two-phase flow characteristics in gas–liquid microreactors. *International Journal of Multiphase Flow*, *32*(7), 791-806.